

REPORT DOCUMENTATION PAGE

Form Approved
OMB No. 0704-01-0188

The public reporting burden for this collection of information is estimated to average 1 hour per response, including the time for reviewing instructions, searching existing data sources, gathering and maintaining the data needed, and completing and reviewing the collection of information. Send comments regarding this burden estimate or any other aspect of this collection of information, including suggestions for reducing the burden to Department of Defense, Washington Headquarters Services, Directorate for Information Operations and Reports (0704-0188), 1215 Jefferson Davis Highway, Suite 1204, Arlington VA 22202-4302. Respondents should be aware that notwithstanding any other provision of law, no person shall be subject to any penalty for failing to comply with a collection of information if it does not display a currently valid OMB control number.

PLEASE DO NOT RETURN YOUR FORM TO THE ABOVE ADDRESS.

1. REPORT DATE (DD-MM-YYYY) 30-10-2007		2. REPORT TYPE REPRINT		3. DATES COVERED (From - To)	
4. TITLE AND SUBTITLE A time-dependent wave packet quantum scattering study of the reaction $HD^+(v=0-3; j_0=1) + He \rightarrow HeH^+(HeD^+) + D(H)$				5a. CONTRACT NUMBER	
				5b. GRANT NUMBER	
				5c. PROGRAM ELEMENT NUMBER 61102F	
				5d. PROJECT NUMBER 2303	
6. AUTHORS Xiaonan Tang*, Cassidy Houchins*, Kai-Chung Lau*, C.Y. Ng*, Rainer A. Dressler, Yu-Hui Chiu, Tian-Shu Chu** and Ke-Li Han				5e. TASK NUMBER RS	
				5f. WORK UNIT NUMBER A1	
				8. PERFORMING ORGANIZATION REPORT NUMBER AFRL-RV-HA-TR-2008-1118	
7. PERFORMING ORGANIZATION NAME(S) AND ADDRESS(ES) Air Force Research Laboratory /RVBXT 29 Randolph Road Hanscom AFB, MA 01731-3010				9. SPONSORING/MONITORING AGENCY NAME(S) AND ADDRESS(ES)	
				10. SPONSOR/MONITOR'S ACRONYM(S) AFRL/RVBXT	
				11. SPONSOR/MONITOR'S REPORT NUMBER(S)	

12. DISTRIBUTION/AVAILABILITY STATEMENT
Approved for Public Release; distribution unlimited.

20081204210

13. SUPPLEMENTARY NOTES
Reprinted from *The Journal of Chemical Physics*, **127**, 164318(2007) © 2007 American Institute of Physics. *University of California, Davis, Davis, CA 95616. **State Key Laboratory of Molecular Dynamics, Dalian Inst. Of Chemical Physics, Dalian 116023, China.

14. ABSTRACT Time-dependent wave packet quantum scattering (TWQS) calculations are presented for $HD^+(v=0, j_0=1) + He$ collisions in the Center-of-mass collision energy (ET) range of 0.0-0.2 eV. The present TWQS approach accounts for Coriolis coupling and uses the *ab initio* potential energy surface of Palmieri et al. [*Mol. Phys.* **98**, 1839 (2000)]. For a fixed total angular momentum J , the energy dependence of reaction probabilities exhibits quantum resonance structure. The resonances are more pronounced for low J values and for the $HeH^+ + D$ channel than for the $HeD^+ + H$ channel and are particularly prominent near threshold. The quantum effects are no longer discernible in the integral cross sections, which compare closely to quasiclassical trajectory calculations conducted on the same potential energy surface. The integral cross sections also compare well to recent state-selected experimental values over the same reactant and translational energy range. Classical impulsive dynamics and steric arguments can account for the significant isotope effect in favor of the deuteron transfer channel observed for $HD^+(v<3)$ and low translational energies. At higher reactant energies, angular momentum constraints favor the proton-transfer channel, and isotopic differences in the integral cross sections are no longer significant. The integral cross sections as well as the J dependence of partial cross sections exhibit a significant alignment effect in favor of collisions with the HD^+ rotational angular momentum vector perpendicular to the Jacobi R coordinate. This effect is most pronounced for the proton-transfer channel at low vibrational and translational energies.

15. SUBJECT TERMS
Coriolis coupling Isotope effect Integral cross-section Proton transfer Quasiclassical trajectory calculation
Time-dependent wave packet quantum scattering

16. SECURITY CLASSIFICATION OF:			17. LIMITATION OF ABSTRACT	18. NUMBER OF PAGES	19a. NAME OF RESPONSIBLE PERSON	
a. REPORT	b. ABSTRACT	c. THIS PAGE			Yu-Hsui Chiu	
UNCL	UNCL	UNCL	UNL		19b. TELEPHONE NUMBER (Include area code)	

DTIC COPY

A time-dependent wave packet quantum scattering study of the reaction $\text{HD}^+(v=0-3; j_0=1) + \text{He} \rightarrow \text{HeH}^+(\text{HeD}^+) + \text{D}(\text{H})$

Xiaonan Tang, Cassidy Houchins, Kai-Chung Lau, and C. Y. Ng^{a)}

Department of Chemistry, University of California, Davis, One Shields Avenue, Davis, California 95616, USA

Rainer A. Dressler^{b)} and Yu-Hui Chiu

Air Force Research Laboratory, Space Vehicles Directorate, Hanscom AFB, Massachusetts 01731-3010, USA

Tian-Shu Chu and Ke-Li Han^{c)}

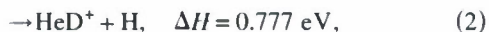
State Key Laboratory of Molecular Reaction Dynamics, Dalian Institute of Chemical Physics, Chinese Academy of Sciences, Dalian 116023, China

(Received 6 August 2007; accepted 26 September 2007; published online 30 October 2007)

Time-dependent wave packet quantum scattering (TWQS) calculations are presented for $\text{HD}^+(v=0-3; j_0=1) + \text{He}$ collisions in the center-of-mass collision energy (E_T) range of 0.0–2.0 eV. The present TWQS approach accounts for Coriolis coupling and uses the *ab initio* potential energy surface of Palmieri *et al.* [Mol. Phys. **98**, 1839 (2000)]. For a fixed total angular momentum J , the energy dependence of reaction probabilities exhibits quantum resonance structure. The resonances are more pronounced for low J values and for the $\text{HeH}^+ + \text{D}$ channel than for the $\text{HeD}^+ + \text{H}$ channel and are particularly prominent near threshold. The quantum effects are no longer discernable in the integral cross sections, which compare closely to quasiclassical trajectory calculations conducted on the same potential energy surface. The integral cross sections also compare well to recent state-selected experimental values over the same reactant and translational energy range. Classical impulsive dynamics and steric arguments can account for the significant isotope effect in favor of the deuteron transfer channel observed for $\text{HD}^+(v < 3)$ and low translational energies. At higher reactant energies, angular momentum constraints favor the proton-transfer channel, and isotopic differences in the integral cross sections are no longer significant. The integral cross sections as well as the J dependence of partial cross sections exhibit a significant alignment effect in favor of collisions with the HD^+ rotational angular momentum vector perpendicular to the Jacobi R coordinate. This effect is most pronounced for the proton-transfer channel at low vibrational and translational energies. © 2007 American Institute of Physics. [DOI: 10.1063/1.2800009]

I. INTRODUCTION

The endothermic $\text{HD}^+ + \text{He}$ reaction to form the isotopologues, HeH^+ and HeD^+ ,



is among the most fundamental chemical reaction systems. It is a textbook example for the study of the translational and internal energy dependences of chemical reactivity. A number of experimental and theoretical studies have investigated isotopic branching in the $\text{HD}^+ + \text{He}$ reactive collision system.^{1–10} Significant discrepancies exist between theory and state-selected studies by Turner *et al.*,⁴ in particular, with regard to the vibrational and translational energy dependences of integral reaction cross section branching ratios, $\Gamma(v) = \sigma_v(\text{HeH}^+)/\sigma_v(\text{HeD}^+)$, for $v=0-4$. More recently, Tang *et al.*¹¹ reported absolute integral proton-transfer and

deuteron transfer cross sections for state-selected reactants, $\text{HD}^+(v, j=1) + \text{He}$, using the vacuum ultraviolet (VUV) photoionization-guided ion beam (VUV-PI-GIB) technique and the pulsed field ionization-photoelectron-secondary ion coincidence scheme. These measurements, which significantly extended the range of reactant vibrational and translational energies for which absolute integral cross sections are available for channels (1) and (2), provided a much improved comparison of determined branching ratios at a translational energy of 1 eV with both quasiclassical trajectory (QCT) as well as time-dependent wave packet quantum scattering (TWQS) calculations by Tiwari *et al.*⁹ The results by Tang *et al.*, therefore, suggest that the measurements by Turner *et al.*, whose branching ratios are approximately a factor of 2 higher than those of Tang *et al.* and Tiwari *et al.* for $v=3$ and 4, are inaccurate. However, the new experimental integral cross sections were in much better agreement with QCT calculations than the TWQS results. Additional quantum studies including high J are, therefore, warranted to resolve the discrepancies.

The $\text{H}_2^+ + \text{He}$ collision system has been the subject of extensive theoretical work.^{7–9, 12–39} Of particular interest has

^{a)}Electronic mail: cyng@chem.ucdavis.edu

^{b)}Electronic mail: afri.rvb.pa@hanscom.af.mil

^{c)}Electronic mail: klhan@dicp.ac.cn

been the observation of prominent resonant structure in the energy dependence of reaction probabilities in quantum scattering experiments.^{7,13,23–34,38} These calculations suggest that the QCT method may not be appropriate in elucidating the dynamics of this fundamental reaction system. A recent accurate potential energy surface calculated by Palmieri *et al.*³⁹ has provided a new impetus to theoretical work on both $\text{H}_2^+ + \text{He}$ reactivity as well as the isotopic $\text{HD}^+ + \text{He}$ reactive channels. Chu *et al.*³⁵ used the Palmieri surface to conduct time-dependent wave packet quantum scattering calculations including Coriolis coupling (TWQS-CC) to determine absolute integral $\text{H}_2^+(v=0-2, 4, 6, j=1) + \text{He}$ proton-transfer cross sections over an unprecedented translational energy range, $E_T = 0-2.4$ eV. Their results demonstrated that the inclusion of the Coriolis coupling is essential for obtaining satisfactory agreement between theoretical and experimental cross sections for $\text{HeH}^+ + \text{H}$ formation from the $\text{H}_2^+ + \text{He}$ reaction. Overall, the TWQS-CC results compared well to the most recent state-selected experiments by Tang *et al.*⁴⁰ This work also demonstrated that despite the prominence of resonances in J -selected reaction probabilities, the TWQS-CC integral cross sections compared very well to QCT calculations using the same potential energy surface.

In this paper, we present a TWQS-CC study of the isotopic reaction channels in $\text{HD}^+(v=0-3; j=1) + \text{He}$ collisions for the collision energy range of 0.0–2.0 eV. A detailed comparison is provided between the present TWQS-CC results, recent experimental work reported by Tang *et al.*,¹¹ and QCT calculations for similar reactant energies.

II. THEORETICAL METHOD

The present TWQS-CC study of reactions (1) and (2) is similar to the recent theoretical investigation of the proton-transfer reaction $\text{H}_2^+(v, j) + \text{He} \rightarrow \text{HeH}^+ + \text{H}$ reported by Chu *et al.*³⁵ The time-dependent wave packet method has been widely used in dynamical studies for the elucidation of the mechanism of simple reactive systems.⁴¹ This method numerically solves the time-dependent Schrödinger equation of the reactive system in conjunction with the split-operator propagator scheme.

In the reactant Jacobi coordinates, the Hamiltonian of the HeHD^+ system can be expressed as

$$H = -\frac{\hbar^2}{2\mu_R} \frac{\partial^2}{\partial R^2} + \frac{(J-j)^2}{2\mu_R R^2} + \frac{j^2}{2\mu_r r^2} + V(\hat{R}, \hat{r}) + h(r), \quad (3)$$

where R is the distance between the center of mass of HD^+ and He, r is the HD^+ bond length, μ_R is the reduced mass of He with respect to HD^+ , μ_r is the HD^+ reduced mass,¹³ J and j are the respective total angular momentum of the $\text{HD}^+ + \text{He}$ reaction system and the rotational angular momentum of HD^+ , $V(\hat{R}, \hat{r})$ is the potential energy surface, as determined by Palmieri *et al.*,³⁹ and $h(r)$ is the diatomic reference Hamiltonian,

$$h(r) = -\frac{\hbar^2}{2\mu_r} \frac{\partial^2}{\partial r^2} + V(r), \quad (4)$$

where $V(r)$ is the diatomic reference potential.

The time-dependent wave function is expanded in terms of the translational basis $U_n^v(R)$, the vibrational basis $\phi_v(r)$, and the body-fixed total angular momentum basis $Y_{jK}^{JM\epsilon}(\hat{R}, \hat{r})$,⁴¹ where M and K are the projection of J on the space-fixed and body-fixed z axis, respectively, and ϵ provides the total parity. In the coupled-state or centrifugal sudden approximation,^{42,43} the matrix obtained by applying the centrifugal potential operator, the second term of the Hamiltonian [Eq. (3)], to the rotational basis functions $Y_{jK}^{JM\epsilon}(\hat{R}, \hat{r})$ is assumed diagonal, whereas in the present CC calculation,^{44,45} different K states are allowed to couple, leading to off-diagonal elements.

The initial wave function is propagated by a split-operator scheme,⁴⁶ and the J , j_0 , k_0 , and v selected reaction probability $[P_{j_0 k_0 v}^J(E_T)]$, the j_0 , k_0 , and v -selected integral reaction cross section $[\sigma_{j_0 k_0 v}(E_T)]$, and the total rovibrationally state-selected integral reaction cross sections $[\sigma_{j_0 v}(E_T)]$ are calculated from⁴¹

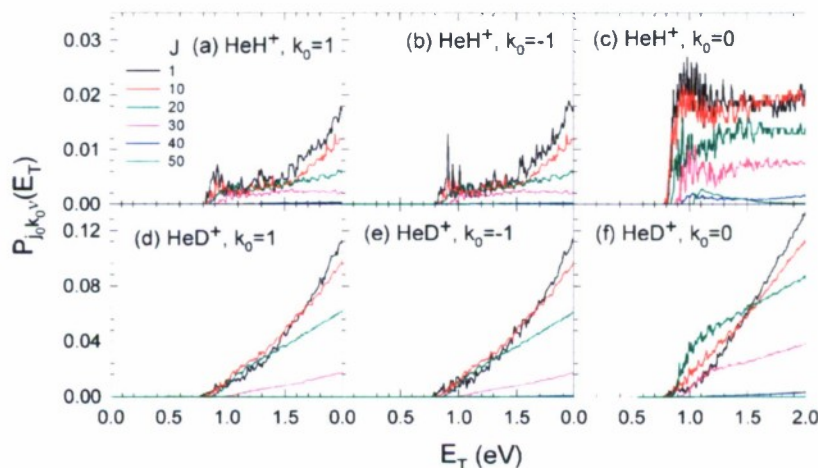


FIG. 1. (Color online) TWQS-CC reaction channel probabilities, $P_{j_0 k_0 v}^J(E_T)$ ($v=0, j_0=1$) for $J=1$ (black curves), 10 (red curves), 20 (green curves), 30 (pink curves), 40 (blue curves), and 50 (dark green curves) in the E_T range of 0.0–2.0 eV for $k_0=0, \pm 1$.

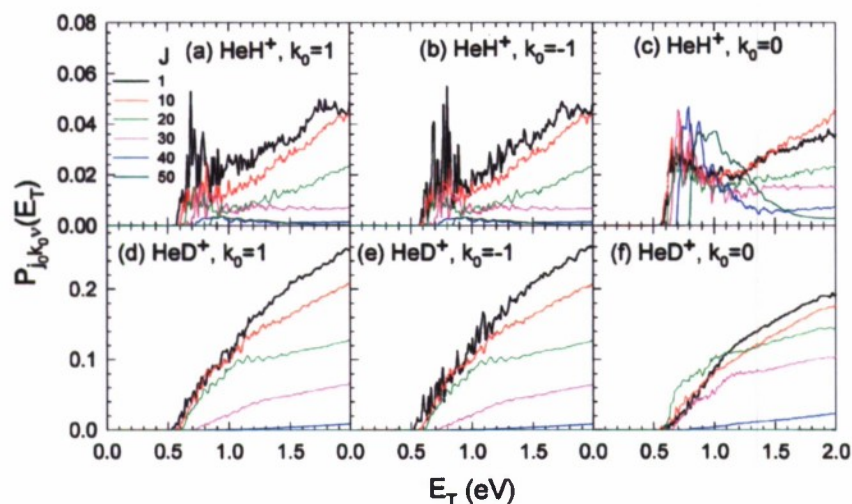


FIG. 2. (Color) TWQS-CC reaction channel probabilities, $P_{j_0k_0v}^J(E_T)$ ($v=1, j_0=1$) for $J=1$ (black curves), 10 (red curves), 20 (green curves), 30 (pink curves), 40 (blue curves), and 50 (dark green curves) in the E_T range of 0.0–2.0 eV for $k_0=0, \pm 1$.

$$P_{j_0k_0v}^J(E_T) = \frac{\hbar}{\mu_r} \text{Im}[\langle \psi(E_T) | \delta(r - r_0) | \psi(E_T) \rangle], \quad (5)$$

$$\sigma_{j_0k_0v}(E_T) = \frac{\pi}{k^2} \sum_J (2J+1) P_{j_0k_0v}^J(E_T), \quad (6)$$

$$\sigma_{j_0v}(E_T) = \frac{1}{2j_0+1} \sum_{k_0} \sigma_{j_0k_0v}(E_T), \quad (7)$$

where $\psi(E_T)$ is the corresponding time-independent part of the final wave function, k_0 is the projection of the initial rotational angular momentum j_0 on the body-fixed z axis, and $k=(2E_T\mu_r/\hbar^2)^{1/2}$ is the wave number corresponding to the initial state at a fixed collision energy, E_T .

The present theoretical work is also complimented with QCT calculations using the same potential energy surface. The present QCT approach has been described previously.^{11,40} While most of the QCT results have been reported already by Tang *et al.*, additional calculations were conducted for those comparisons where higher statistics were necessary. Up to 90 000 trajectories were computed in those cases.

III. RESULTS

A. Reaction probabilities

Figures 1(a)–1(c) [1(d)–1(f)] depict the translational energy dependencies between 0 and 2.0 eV of the TWQS-CC reaction probabilities $P_{j_0k_0v}^J(E_T)$ for the formation of HeH⁺ [HeD⁺] calculated with HD⁺ in the respective ($v=0$; $j_0=1$, $k_0=0, \pm 1$) states at $J=1$ (black curves), 10 (red curves), 20 (green curves), 30 (pink curves), 40 (blue curves), and 50 (dark green curves). The corresponding translational energy dependencies of TWQS-CC reaction probabilities for $v=1, 2$, and 3 calculated for the same J values are compared in Figs. 2–4, respectively.

Sharp resonance structure is observed, particularly for $J=1$ collisions near threshold. As J is increased, the resonance structure becomes less evident. Reactive resonances are more pronounced for HeH⁺ than for HeD⁺. The general trends of the probabilities with energy are also quite different for the two isotopic channels. The reaction probabilities for HeD⁺ increase gradually as a function of E_T except near the probability maximum of $J \approx 20$, whereas the probabilities for HeH⁺ generally have a sharper onset at threshold, above which the resonances are the most pronounced. For a fixed reactant vibrational level and a fixed J value, the behaviors

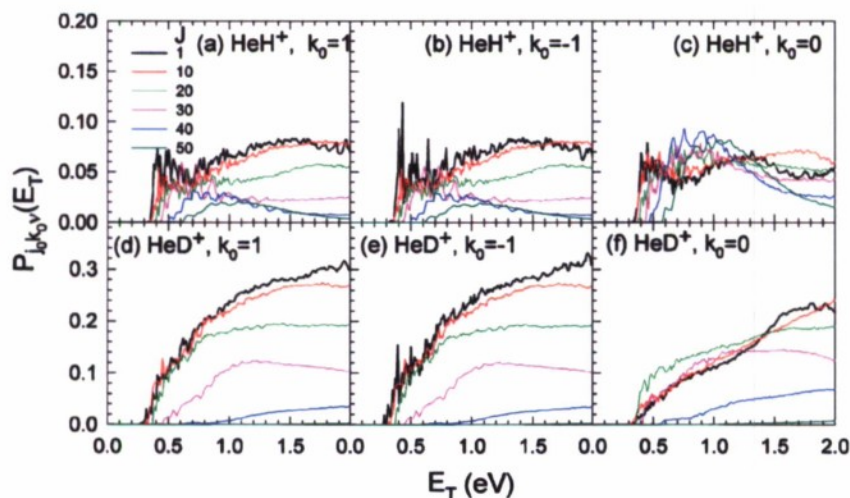


FIG. 3. (Color) TWQS-CC reaction channel probabilities, $P_{j_0k_0v}^J(E_T)$ ($v=2, j_0=1$) for $J=1$ (black curves), 10 (red curves), 20 (green curves), 30 (pink curves), 40 (blue curves), and 50 (dark green curves) in the E_T range of 0.0–2.0 eV for $k_0=0, \pm 1$.

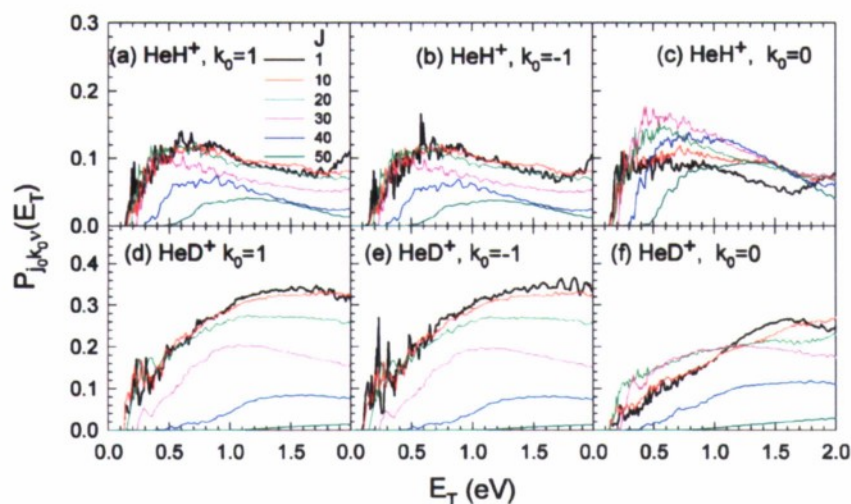


FIG. 4. (Color) TWQS-CC reaction channel probabilities, $P_{j_0 k_0 v}^J(E_T)$ ($v=3, j_0=1$) for $J=1$ (black curves), 10 (red curves), 20 (green curves), 30 (pink curves), 40 (blue curves), and 50 (dark green curves) in the E_T range of 0.0–2.0 eV for $k_0=0, \pm 1$.

of the reaction probabilities for $k_0=1$ and $k_0=-1$ are similar, but are substantially different from the behavior for $k_0=0$ reactants. The probability curves of both channels calculated for $k_0=\pm 1$ and $v=0-3$ are shown to decrease as J is increased, whereas the $k_0=0$ probability curves of HeD^+ for $v=0-3$ and HeH^+ for $v=1-3$ have considerable contributions from high J collisions. We note that since the reaction cross section is associated with a reaction probability scaled by $(2J+1)$, the contribution to the reaction cross sections from higher J values is larger than appears from the reaction probabilities. Furthermore, for all k_0 and J values, the E_T onset for the $P_{j_0 k_0 v}^J(E_T)$ curve appears to increase as J is increased. This trend is more pronounced as the reactant vibrational energy increases.

A more comprehensive three dimensional (3D) representation of $P_{j_0 k_0 v}^J(J, E_T)$ is shown for $v=0$ and 1 reactant ions in Figs. 5 and 6, respectively. The $k_0=-1$ states are not shown because they are very similar to the corresponding plots for $k_0=1$ states. The 3D graphs reaffirm the above observation

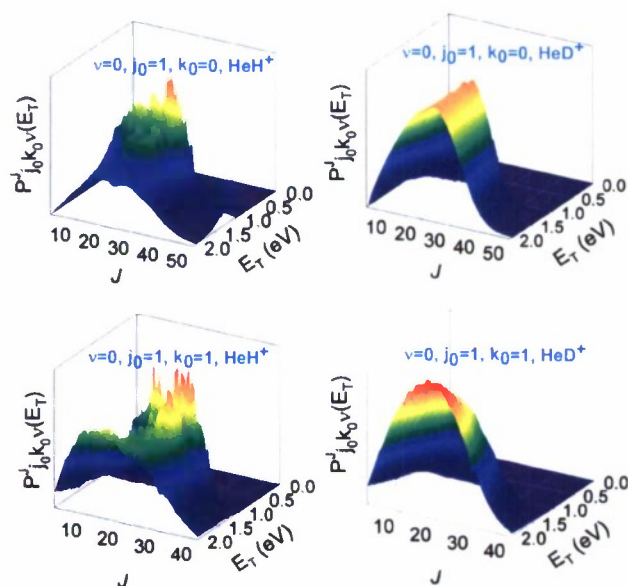


FIG. 5. (Color) The reaction probabilities $P_{j_0 k_0 v}^J(J, E_T)$ ($v=0, j_0=1, k_0=0, \pm 1$) for HeH^+ +D and HeD^+ +H formation plotted as a function of J and E_T .

that reactive resonances are significantly sharper and more pronounced for the HeH^+ channel. The resonance structure diminishes as v is increased from 0 to 3. Corresponding plots for $v=2$ and $v=3$ can be obtained from the authors.

B. J dependence of partial cross sections

The proton or deuteron transfer TWQS-CC partial cross sections for a given reactant state $\text{HD}^+(v, j_0, k_0)$, $\sigma_{j_0 k_0 v}^J(J, E_T) = (\pi/k^2)(2J+1)P_{j_0 k_0 v}^J(E_T)$, depend on both J and E_T . Figure 7 exhibits the J dependencies of the respective partial cross sections for $v=0-3; j_0=1, k_0=0, \pm 1$ at $E_T=1$ eV for the two isotopic channels. These partial cross section plots show that the theoretical partial cross sections for $k_0=1$ and -1 are essentially identical and that the TWQS-CC cross sections at $E_T=1$ eV vanish above $J \approx 70$. A significant preference for $k_0=0$ reactants is observed in the HeH^+ +D channel for all investigated reactant states and for $v=0$ reactants in the HeD^+ +H channel. For $v>0$ reactants, the HeD^+ +H partial cross sections at 1 eV are nearly indepen-

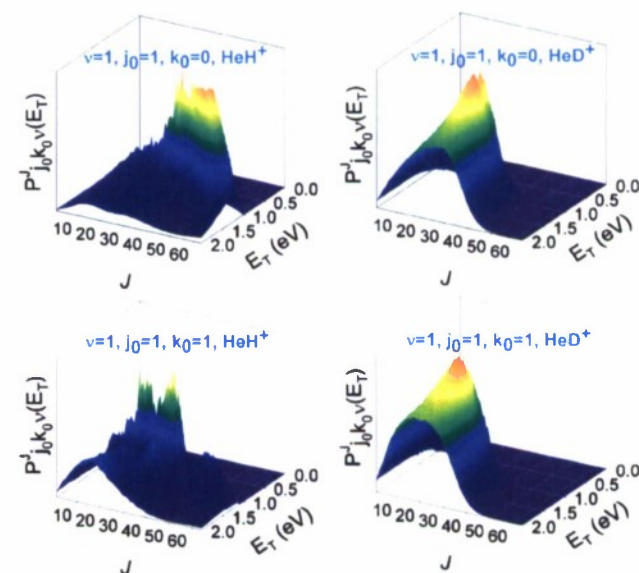


FIG. 6. (Color) The reaction probabilities $P_{j_0 k_0 v}^J(J, E_T)$ ($v=1, j_0=1, k_0=0, \pm 1$) for HeH^+ +D and HeD^+ +H formation plotted as a function of J and E_T .

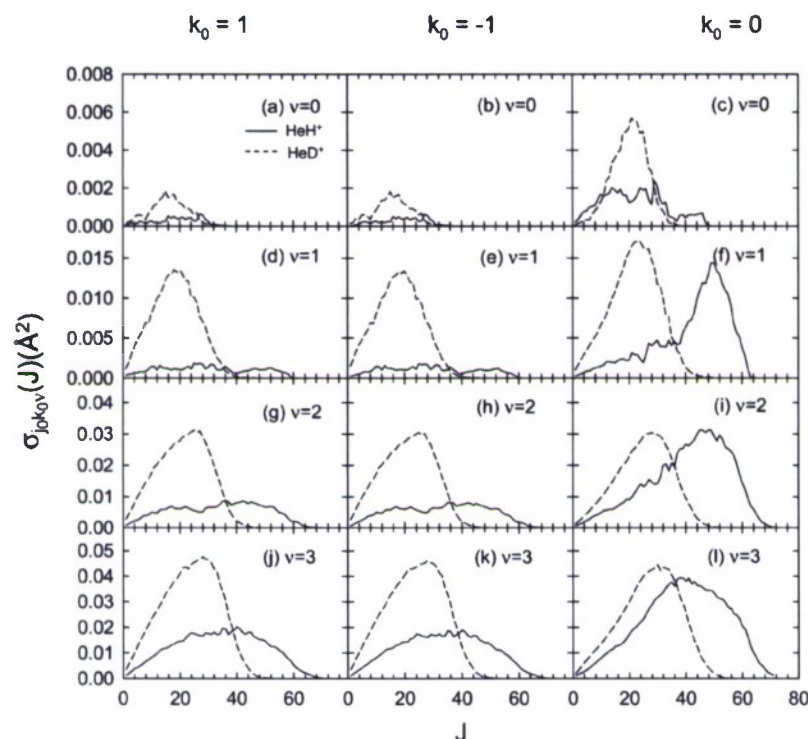


FIG. 7. J dependencies of the TWQS-CC partial cross sections, $\sigma_{j_0 k_0 v}(J, E_T)$ ($j_0=1, E_T=1$ eV) for $v=0-3$, and $k_0=0, \pm 1$ for the formation of HeH⁺ (solid curves) and HeD⁺ (dashed curves).

dent of k_0 . As expected, given the endothermicity of the reaction, the TWQS-CC partial cross sections for HeH⁺ and HeD⁺ increase significantly as v increases. There is a gradual shift of the J distribution to higher values as v increases. Furthermore, except for $v=0$ reactants, there is a clear preference for HeD⁺ formation at low J values, whereas the formation of HeH⁺ is favored at high J values. The cross-over J value above which the HeH⁺ channel is preferred occurs between 35 and 40 and does not show a clear dependence on v for $v=1-3$.

Figure 8 compares the k_0 -averaged TWQS-CC partial cross sections with QCT calculations based on the same potential energy surface by Palmieri *et al.*³⁹ The previous comparison between experimental and QCT integral cross sections¹¹ has demonstrated that the agreement is most favorable if the zero-point energy in reaction products is disregarded. In this work, we consequently only compare with QCT calculations that do not account for product zero-point energy. The absolute QCT values, shown as solid and dashed lines for HeH⁺ and HeD⁺, respectively, are derived from $\hbar \partial \sigma_{j_0 v}(L) / \partial L$, where $L = \mu_r g b$ is the classical correspondence to $L^2 \approx J(J+1)\hbar^2$ assuming $J = |l+j| \approx l$, and g and b are the relative velocities at infinite distance and impact parameter, respectively. There is generally a good agreement between the classical and TWQS-CC partial cross sections, both in magnitude and J dependence. The classical distributions exhibit a minor shift toward higher angular momentum collisions in both channels. Probably the most significant differences between TWQS-CC and QCT are seen in the HeH⁺ channel for $v=0$ reactants, where unlike QCT, the TWQS-CC results exhibit bimodality with a tail toward high J .

C. Rovibrationally state-selected integral cross sections

The TWQS-CC integral cross sections, $\sigma_{j_0 k_0 v}(E_T, v=0-3; j_0=1; k_0=0, \pm 1)$, for both isotopic channels calculated for $E_T=0.0-2.0$ eV are plotted in Fig. 9. The solid curves shown in these figures are the k_0 -averaged, rovibrationally state-selected integral cross sections, $\sigma_{j_0 v}(E_T)$. It is seen that the $k_0=0$ integral cross sections for HeD⁺ and HeH⁺ are larger than the corresponding $k_0=\pm 1$ cross sections over the whole E_T range except the HeD⁺ values for $v=2$ and 3, where the cross sections are observed to be essentially independent of k_0 . All the cross section curves exhibit relatively sharp E_T thresholds. The pronounced resonance structure observed in the probability curves is greatly suppressed in the TWQS-CC integral cross sections due to J and k_0 averaging. With the exception of the $v=0$ integral cross sections of the HeD⁺ channel [Fig. 9(a)], which still increase at $E_T=2$ eV, the HeD⁺ integral cross sections for reactant states $v=1-3$ [Figs. 9(b)–9(d)] and those of HeH⁺ for $v=0-3$ [Figs. 9(aa)–9(dd)] are found to decline at energies above 1 eV. The decline is found to be more rapid in the case of HeH⁺ formation. Also, the integral reaction cross sections for the HeH⁺ isotopic channel display sharper maxima. Interestingly, the HeD⁺ cross sections for $v=1-3$ reactants [Figs. 9(b)–9(d)] manifest some structure near threshold.

Figure 9 also compares the k_0 -averaged TWQS-CC cross sections with QCT calculations using the surface by Palmieri *et al.*³⁹ Except close to threshold, the QCT predictions are generally in very good agreement with the TWQS-CC results. The discrepancy at threshold is expected because zero-point energy of product molecular ions is not taken into

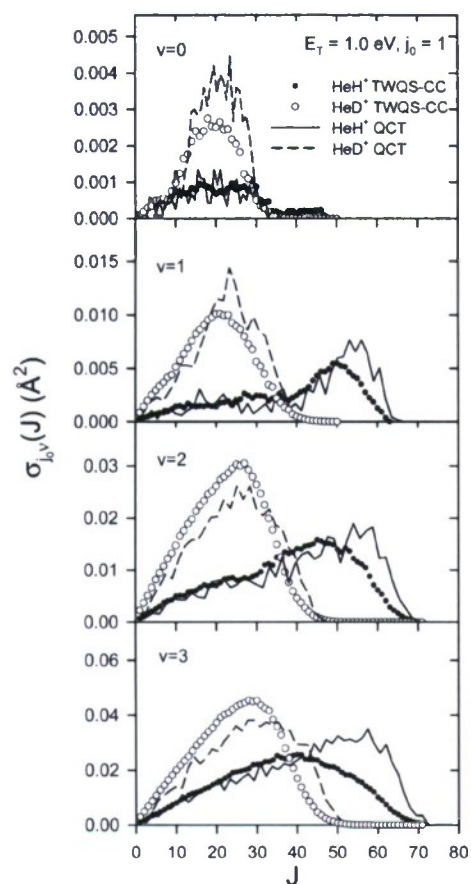


FIG. 8. k_0 -averaged TWQS-CC partial cross sections $\sigma_{J(v)}(J)$ for $E_T=1$ eV, $j_0=1$, and $v=0-3$ (filled circles: $\text{HeH}^+ + \text{D}$; open circles: $\text{HeD}^+ + \text{H}$). The solid and broken lines are the corresponding QCT results, $\hbar \partial \sigma_{j_0}(L) / \partial L$.

account in the QCT calculations. Consequently, the QCT thresholds are not just lower than the exact thresholds, but are identical for the two isotopic channels.

D. Comparison with experimental cross sections

A detailed comparison of existing experimental and theoretical cross sections for reactions (1) and (2) was recently reported by Tang *et al.*¹¹ In Fig. 10 we compare the VUV-PI-GIB measurements of integral reaction cross sections reported by Tang *et al.* to the present TWQS-CC results. The theoretical cross section energy dependence has been convoluted by the experimental energy broadening functions, including both thermal target gas broadening⁴⁷ and the ion energy resolution of the experiment (~ 0.3 eV). Any structure observed in the TWQS-CC cross section energy dependencies, particularly the shoulder observed in the HeD^+ onsets, is no longer apparent following the convolution. Above 1 eV, the agreement between experimental and theoretical cross sections is excellent. At lower energies, the experimental values are slightly higher than the theoretical predictions, particularly near the cross section maxima for $v=1$ and 2. For all reactant states, the energy regions of strong cross section growth with energy appear at slightly higher energies

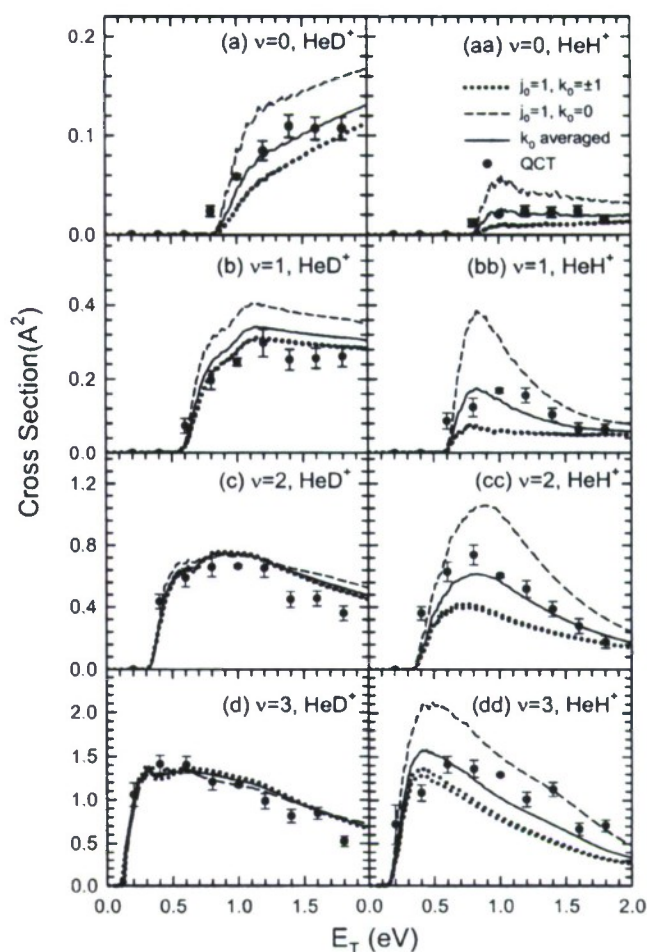


FIG. 9. The TWQS-CC proton and deuteron transfer integral cross sections $\sigma_{J(v)}(E_T)$ with $j_0=1$ and $k_0=0$ (dashed line), ± 1 (dotted lines), and k_0 -averaged (solid line) in the E_T range of 0.0–2.0 eV for $v=0-3$. The TWQS-CC results are compared with QCT cross sections.

in the case of the theoretical results. This shift in apparent cross section onset is more pronounced in the case of the deuteron transfer channel.

The source of the discrepancy near threshold could be caused by translational energy calibration error in the experiments, or by differences in the steepness of the experimental and theoretical threshold onsets, or by inaccuracies in the potential energy surface. Tang *et al.*¹¹ found that the observed cross section energy dependences for the four lowest reactant vibrational states were consistent with modified line-of-center^{48,49} threshold functions based on the known thermochemical thresholds of the two isotopic channels. The deconvoluted cross sections, however, were found to have highly vertical onsets at threshold. A difference in threshold function steepness could also be related to the fact that the VUV-PI-GIB measurements by Tang *et al.* were not rotationally state selected, unlike the TWQS-CC calculations which were conducted for $j_0=1$. This is further discussed in the next section.

Table I compares the branching ratios $\Gamma(v)$ derived from the present calculations at 1 eV to those obtained from the present QCT calculations and other theoretical work, as well as experimental values. The TWQS-CC results are in good

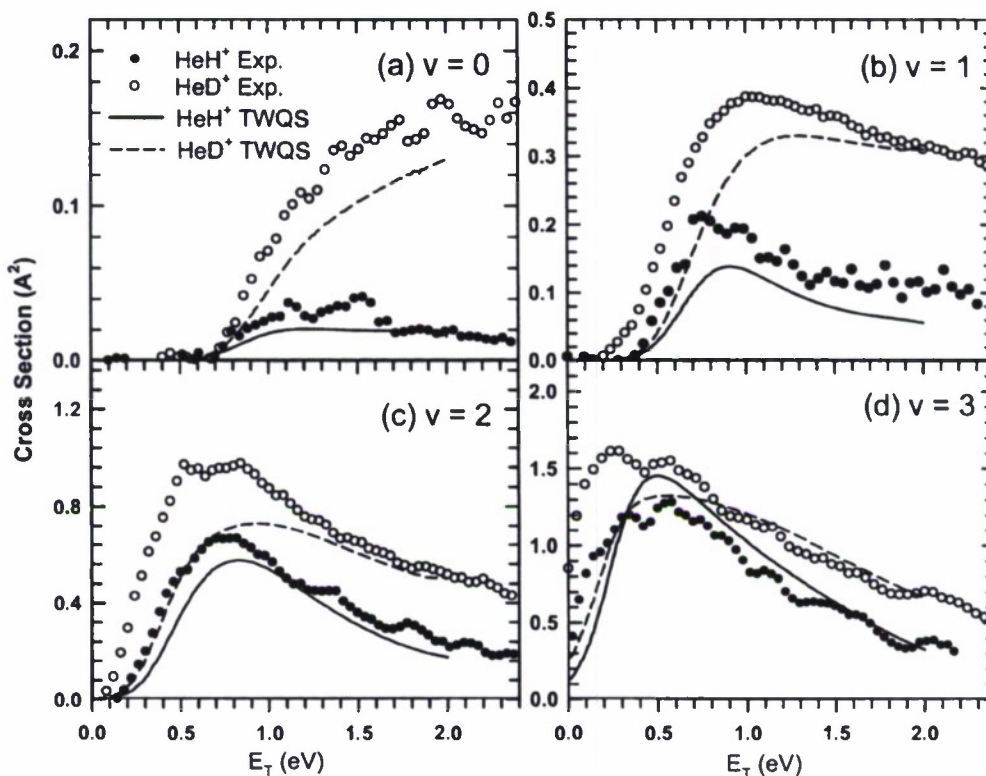


FIG. 10. Comparison between the energy dependence of experimental (filled and open circles) and TWQS-CC (solid and dashed lines) integral reaction cross sections. The TWQS-CC curves have been convoluted by the experimental energy broadening function, including primary ion energy distribution and target gas thermal motion.

agreement with the experimental values apart from slightly higher values at $v=0$ and 2. Except at $v=0$, the present QCT results have higher ratios than those produced by TWQS-CC. The TWQS branching ratios by Tiwari *et al.*⁹ are significantly different from the experimental ones for $v < 2$.

IV. DISCUSSION

The present work confirms the accuracy of the TWQS-CC method in predicting accurate integral cross sections for the textbook $\text{H}_2^+(\text{HD}^+) + \text{He}$ reaction systems at total energies as high as 2.8 eV using the potential energy surface of Palmieri *et al.*³⁹ The isotopic branching in the present study is a particularly sensitive probe of the dynamics. As

seen in Table I and Fig. 10, the calculations are successful in reproducing the vibrationally state-selected experimental integral cross sections and respective isotopic ratios by Tang *et al.*¹¹ at translational energies above 1 eV. Closer to threshold, the calculations appear to underpredict the $v=2$ and 3 HeD⁺ channel cross sections; however, the theoretical results are still within the stated experimental accuracy. The latter is reduced near threshold due to the relatively broad experimental translational energy distribution in a region of strong cross section energy dependence. As mentioned in the previous section, Tang *et al.*¹¹ deconvoluted the experimental cross sections to derive modified line-of-center threshold functions that have significantly steeper onsets than predicted by the present theory. Assuming that no translational calibra-

TABLE I. Comparison of the experimental and theoretical values for the branching ratios $\Gamma(v) = \sigma_v(\text{HeH}^+)/\sigma_v(\text{HeD}^+)$ ($v=0-3$) obtained at $E_T=1.0$ eV, where $\sigma_v(\text{HeH}^+)$ and $\sigma_v(\text{HeD}^+)$ are integral cross sections for the formation of HeH⁺ and HeD⁺ respectively.

HD ⁺ (v) state	Experiment ^a		Theory				
			TWQS-CC ^b	TWQS ^c	QCT ^b	QCT ^d	TSH ^e
$v=0$	0.39	0.98	0.54	1.06	0.35±0.04	0.34	0.75
$v=1$	0.51	0.72	0.47	0.23	0.69±0.06	0.92	0.33
$v=2$	0.57	1.04	0.77	0.52	0.91±0.04	0.92	0.71
$v=3$	0.70	1.38	0.83	0.83	1.11±0.04	1.20	1.20

^aLeft: Ref. 11; right: Ref. 4.

^bPresent.

^cReference 9.

^dReference 5.

^eReference 6.

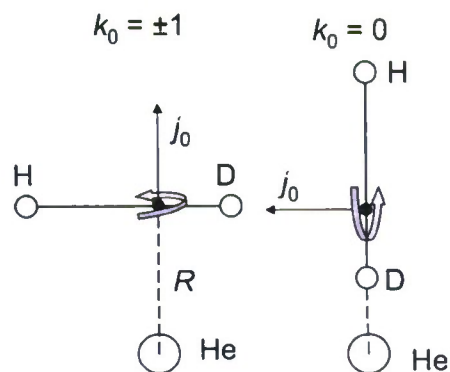


FIG. 11. Schematic illustration of $j_0=1$ projections, $k_0=0, \pm 1$, where R is the quantization axis.

tion error is the cause of the discrepancy, it is possible that the population of reactant rotational states $j_0 \neq 1$ in the experiments and a particular sensitivity to reactant rotational energy is responsible for the steeper experimental onset. Indeed, Kalyanaraman *et al.*⁸ discovered a strong j_0 dependence of $J=0$ reaction probabilities in quantum scattering calculations. They found that the $\text{HeH}^+ + \text{D}$ channel j_0 dependence was irregular with v , while the $\text{HeD}^+ + \text{H}$ channel exhibited a preference for even j_0 quantum numbers for all v , with $j_0=1$ reactants exhibiting the lowest probabilities. Subsequently, Tiwari and Sathyamurthy¹⁰ calculated the rotational energy dependence of integral cross sections for $v=1$ reactants using a three dimensional TWQS approach. Their results show that in the case of the proton-transfer channel, $j_0=1$ cross sections are slightly lower than those for $j_0=0$, but significantly higher than $j_0=2$ and 3, while the deuteron transfer cross sections of $j_0=1$ reactants are substantially lower than those of $j_0=0, 2$, and 3. This observation would be consistent with observation that the theoretical $j_0=1$ deuteron transfer channel cross sections exhibit larger differences with the experimental cross sections than the proton-transfer results near threshold.

Additional evidence for reactant rotational sensitivity is provided by the significant k_0 dependence of the $\text{HeH}^+ + \text{D}$ channel integral state-selected cross sections at all investigated reactant vibrational levels and for $v=0$ and 1 reactants for the HeD^+ channel (Fig. 9). Similar observations were made by Tiwari and Sathyamurthy for $v=1$ reactants.¹⁰ The favoring of $k_0=0$ reactants signifies a preferred reactant alignment with the HD^+ rotational axis perpendicular to the Jacobi R coordinate, represented by the line between the He target and the HD^+ center of mass. This is shown schematically in Fig. 11 for collisions at the point of approach, $R \approx 0.7 \text{ \AA}$, which is also the equilibrium distance between the H atom and the center of mass of HD^+ . The preference of $k_0=0$ is consistent with the minimum energy reaction path proceeding through a collinear geometry.

In Fig. 7, it is seen that at 1 eV, the $v=0, k_0=0$ partial cross sections of both isotopic channels are largest near $J=20$ which corresponds to an impact parameter of $\sim 0.7 \text{ \AA}$. For $k_0=\pm 1$, the distributions peak near $J=15$. At all $k_0, v=0$ reactants preferably form $\text{HeD}^+ + \text{H}$ products. This is consistent with the necessity to transfer $\sim 80\%$ of the transla-

tional energy into internal energy through small impact parameter collisions, whereby the impact parameters have to be slightly smaller for the $k_0=\pm 1$ rotational orientations for H/D atoms to undergo sufficiently close interaction with the He target atom.

The excellent agreement between QCT and the present quantum calculations suggests that the minor difference in isotopic thresholds only plays a role in the preference for $\text{HeD}^+ + \text{He}$ products at energies above threshold comparable to the isotopic difference. The favoring of the deuteron transfer channel can be much more readily explained using energy transfer arguments associated with impulsive or spectator-stripping-type dynamics. Tang *et al.*¹¹ interpreted recoil velocity distributions observed for $v=3$ reactants at $E_T=0.6 \text{ eV}$, as evidence for an impulsive or spectator-stripping mechanism. In a purely impulsive mechanism in which only the transferred proton/deuteron collides with the He target atom, 47% of the translational energy is transferred into the product ion in the case of the proton-transfer channel, while 78% is transferred in the case of the deuteron transfer channel. Thus, for endothermic processes, a direct mechanism would strongly favor the $\text{HeD}^+ + \text{H}$ products. In the case of the high-threshold $v=0$ process, additional favoring of the deuteron transfer channel may be attributable to the on average closer He–D distance at the turning point of the collision given the tighter gyrating trajectory of the D atom due to its closer vicinity to the center of mass of the rotating HD^+ molecule.

For $v=1$ reactants, the HeH^+ channel is preferred by higher J collisions with still a strong preference for the $k_0=0$ rotational alignment, while the alignment effect is less pronounced for the HeD^+ channel (see Fig. 7). For the latter, the partial cross sections still peak around $J=20$, with the $k_0=0$ distribution at slightly higher J than the $k_0=\pm 1$ distributions. As pointed out by Tang *et al.*,¹¹ the significant difference in the opacity functions of the two isotopic channels can be rationalized by the significant difference in the reduced mass of the two product channels coupled with the steric argument of the longer reach of the H atom with respect to the HD^+ center of mass. While the $\text{HeH}^+ + \text{D}$ channel has a reduced mass of 1.43 amu that is similar to that of the reactants (1.71 amu), the reduced mass of $\text{HeD}^+ + \text{H}$ products is significantly lower (0.86 amu) than those of the reactants, and thus, substantial angular momentum conservation constraints arise at large J for the deuteron transfer channel. Interestingly, Light and Lin have predicted this large isotope effect in the opacity functions for this reaction due to angular momentum conservation arguments more than 40 years ago.¹

The large preference for $k_0=0$ reactants in the HeH^+ channel can be explained by the higher probability of transferring sufficient energy in the large impact parameter collisions that appear to be dynamically preferred by this channel. This is also seen to be the case for $v=2$ and 3 reactants. However, in the case of $\text{HeD}^+ + \text{H}$ products, there is no longer a significant difference between the k_0 -selected integral cross sections, and only a minor shift in the J distributions is observed. This is consistent with a J distribution that is primarily dictated by angular momentum constraints versus energy transfer requirements. The latter are not as strin-

gent for the deuteron transfer channel due to the higher efficiency in impulsive dynamics. The present classical rationalization is further justified by the close resemblance of the k_0 -averaged partial cross section distributions and corresponding QCT results shown in Fig. 8. Qualitatively, the partial cross sections calculated by Tiwari *et al.*^{9,10} using TWQS with both the Palmieri *et al.*³⁹ and McLaughlin-Thompson-Joseph-Sathyamurthy^{15,50} potential energy surfaces are similar to the present distributions; however, the present calculations including Coriolis coupling resemble the QCT predictions more closely at $E_T=1$ eV.

Consistency with the above interpretations is also found with the overall behavior of the translational energy dependence of the J -dependent reaction probabilities shown in Figs. 1–6. Three types of dynamics can be identified: Sharp onsets at threshold; dynamics associated with a steady increase followed by a decrease (if extended to a sufficiently high E_T) in cross section with energy; and dynamics associated with resonance-type structure. Where a steady increase in cross section with energy is observed, this behavior turns on at lower energies in the case of the HeD⁺+H channel, which is consistent with impulsive dynamics and the higher efficiency in energy transfer for this channel. Sharp resonance structure due to quantum effects is prominent near threshold. This structure is particularly evident in the case of the HeH⁺ channel where the total probabilities are significantly lower. Interestingly, the resonances are sharper and more intense for low J , $k_0=\pm 1$ collisions, suggesting that they are less likely to be associated with the attractive well found in the collinear geometry. The resonances are more likely attributable to trajectories with a T-type entrance geometry that are associated with a barrier. In this geometry, the interaction of He is more likely to involve both H and D, contrary to more impulsive dynamics involving interaction between the He atom and a single atom of the HD⁺ reactants in the collinear $k_0=0$ geometry. The broader resonances observed for both channels at higher J and v at all orientations are symptomatic of shorter-lived intermediates. As already pointed out by Light and Lin,¹ statistical density of state arguments favor the deuteron transfer channel. Thus, the decay of transition state resonances would occur more rapidly toward deuteron transfer products, explaining the broader resonances, while longer-lived resonances in a highly indirect mechanism provide more efficient energy transfer in the proton-transfer channel. For the latter, differences are observed between $k_0=+1$ and -1 scattering in the detailed positions of the quantum scattering resonance peaks, suggesting orientation effects at this level of detail.

As shown in Fig. 9, resonances do not appear to have an important effect on the overall reactivity given the very good agreement between the k_0 -averaged quantum and QCT integral cross sections. This is not too surprising given the fact that the resonances are most prominent for low J collisions, which do not contribute strongly to the integral cross section. The fact that the QCT calculations that do not take zero-point energy into account compare so well to the present TWQS-CC calculations further suggests that the observed isotope effects shortly above threshold have a purely dy-

namic origin and that the reaction threshold difference, which is zero for the QCT calculations, is only of importance at and immediately above threshold.

V. CONCLUSIONS

We have carried out a 3D TWQS-CC calculation for the rovibrationally state-selected isotopic reactions HD⁺ ($v=0-3; j_0=1$)+He→HeH⁺(HeD⁺)+D (H) in the E_T range of 0.0–2.0 eV using the *ab initio* potential energy surface of Palmieri *et al.*³⁹ Particular attention was paid to the rotational orientation with respect to the body-fixed z axis. The results are compared with QCT calculations on the same potential energy surface and the state-selected experiments by Tang *et al.*¹¹ TWQS-CC k_0 -averaged integral cross sections compare closely to QCT predictions over most of the investigated translational energy range, with only important discrepancies near threshold. The k_0 -averaged partial cross sections $\sigma_{j_0v}(J)$ at 1 eV are also in good qualitative agreement with QCT predictions, suggesting that most of the salient dynamics can be explained with classical arguments. The TWQS-CC integral cross sections are compared to state-selected experiments by Tang *et al.*¹¹ following convolution of the quantum results by the respective experimental energy distribution function. Above threshold, there is excellent agreement between the experimental and theoretical results. The experimental energy region of strong cross section growth with energy, however, is slightly shifted to lower energies than the corresponding convoluted theoretical values. This could be attributed to a lower steepness of the theoretical cross section onset, possibly attributable to important rotational effects given the fact that the experiment included contributions from thermally populated $j_0 \neq 1$ reactant states.

TWQS-CC, QCT, and experiment demonstrate a significant isotope effect for $v < 3$ favoring the deuteron transfer channel. The isotope effect is primarily the result of competition between impulsive dynamics favoring the deuteron transfer channel in case of high-threshold processes, and angular momentum constraints favoring proton-transfer reactions at high J . Consequently, indirect dynamics, including quantum scattering resonances, play an important role in the HeH⁺+D channel near threshold, where impulsive dynamics are inhibited due to inefficient translational-to-internal energy transfer. At high total energy, the two sources for opposite isotope effect balance and branching ratios are close to 1.

TWQS-CC integral cross sections predict a significant alignment effect, favoring k_0 reactants for $v=0-3$ in the HeH⁺+D channel and for $v=0$ and 1 in the HeD⁺+H channel. The alignment effects are consistent with classical steric arguments favoring a collinear approach geometry, angular momentum conservation constraints, and energy transfer differences in impulsive dynamics. The calculated J and energy dependent reaction probabilities are consistent with this picture apart from significant quantum scattering resonances.

ACKNOWLEDGMENTS

This work has been supported by AFOSR through task 2303EP02 and Grant No. F49620-99-1-0234 (Program Man-

ager, Michael R. Berman). C.Y.N. also acknowledges the support of AFOSR Grant No. FA9550-06-1-0073, the NSF Grant Nos. ATM-0317422 and CHE-0517871, and the DOE Grant No. DE-FG02-02ER15306. K.L.H. acknowledges the support of NKBRFSF (2007CB815202), the Knowledge Innovation Program of the Chinese Academy of Sciences (INF105-SCE-02-08), and NSFC (20373071 and 20333050). The calculations of this work were performed using the resources of the National Energy Research Scientific Computing Center supported by the Office of Science of the U.S. Department of Energy under Contract No. DE-AC03-76SF00098; and the Molecular Science Computing Facility (MSCF) in the William R. Wiley Environmental Molecular Sciences Laboratory sponsored by the U.S. Department of Energy's Office of Biological and Environmental Research.

- ¹J. C. Light and J. Lin, *J. Chem. Phys.* **43**, 3209 (1965).
- ²F. S. Klein and L. Friedman, *J. Chem. Phys.* **41**, 1789 (1964).
- ³M. A. Berta, B. Y. Ellis, and W. S. Koski, *J. Chem. Phys.* **44**, 4612 (1966).
- ⁴T. Turner, O. Dutuit, and Y. T. Lee, *J. Chem. Phys.* **81**, 3475 (1984).
- ⁵K. C. Bhalla and N. Sathyamurthy, *Chem. Phys. Lett.* **160**, 437 (1989).
- ⁶K. Dong, E. A. Gislason, and M. Sizun, *Chem. Phys.* **179**, 143 (1994).
- ⁷S. Mahapatra and N. Sathyamurthy, *J. Chem. Phys.* **105**, 10934 (1996).
- ⁸C. Kalyanaraman, D. C. Clary, and N. Sathyamurthy, *J. Chem. Phys.* **111**, 10910 (1999).
- ⁹A. K. Tiwari, A. N. Panda, and N. Sathyamurthy, *J. Phys. Chem. A* **110**, 389 (2006).
- ¹⁰A. K. Tiwari and N. Sathyamurthy, *J. Phys. Chem. A* **110**, 11200 (2006).
- ¹¹X. N. Tang, H. Xu, C. Houchins, C. Y. Ng, Y. Chiu, R. A. Dressler, and D. J. Levandier, *J. Chem. Phys.* **126**, 234305 (2007).
- ¹²M. Sizun and E. A. Gislason, *J. Chem. Phys.* **91**, 4603 (1989).
- ¹³J. T. Adams, *Chem. Phys.* **33**, 275 (1975).
- ¹⁴T. Joseph and N. Sathyamurthy, *J. Chem. Phys.* **86**, 704 (1987).
- ¹⁵T. Joseph and N. Sathyamurthy, *J. Chem. Phys.* **80**, 5332 (1987).
- ¹⁶S. Kumar, H. Kapoor, and N. Sathyamurthy, *Chem. Phys. Lett.* **289**, 361 (1998).
- ¹⁷N. Sathyamurthy, *Chem. Phys. Lett.* **59**, 95 (1978).
- ¹⁸N. Sathyamurthy, *Chem. Phys.* **62**, 1 (1981).
- ¹⁹N. Sathyamurthy and L. M. Raff, *J. Chem. Phys.* **63**, 464 (1975).
- ²⁰N. Sathyamurthy, R. Rangarajan, and L. M. Raff, *J. Chem. Phys.* **64**, 4606 (1976).
- ²¹C. Zuhrt, F. Schneider, U. Havemann, L. Züllicke, and Z. Herman, *Chem. Phys.* **38**, 205 (1979).
- ²²N. Balakrishnan and N. Sathyamurthy, *Comput. Phys. Commun.* **63**, 209 (1991).
- ²³N. Balakrishnan and N. Sathyamurthy, *Chem. Phys. Lett.* **201**, 294 (1993).
- ²⁴N. Balakrishnan and N. Sathyamurthy, *Chem. Phys. Lett.* **240**, 119 (1995).
- ²⁵T. Joseph and N. Sathyamurthy, *J. Indian Chem. Soc.* **62**, 874 (1985).
- ²⁶D. J. Kouri and M. Baer, *Chem. Phys. Lett.* **24**, 37 (1974).
- ²⁷S. Mahapatra and N. Sathyamurthy, *J. Chem. Phys.* **102**, 6057 (1995).
- ²⁸K. Sakimoto and K. Onda, *Chem. Phys. Lett.* **226**, 227 (1994).
- ²⁹N. Sathyamurthy, M. Baer, and T. Joseph, *Chem. Phys.* **114**, 73 (1987).
- ³⁰B. Lepetit and J. M. Launay, *J. Chem. Phys.* **95**, 5159 (1991).
- ³¹S. Mahapatra and N. Sathyamurthy, *J. Chem. Phys.* **107**, 6621 (1997).
- ³²B. Maiti, C. Kalyanaraman, A. Panda, and N. Sathyamurthy, *J. Chem. Phys.* **117**, 9719 (2002).
- ³³B. Maiti, S. Mahapatra, and N. Sathyamurthy, *J. Chem. Phys.* **113**, 59 (2000).
- ³⁴J. Z. H. Zhang, D. L. Yeager, and W. H. Miller, *Chem. Phys. Lett.* **173**, 489 (1990).
- ³⁵T.-S. Chu, R.-F. Lu, K.-L. Han, X.-N. Tang, H.-F. Xu, and C. Y. Ng, *J. Chem. Phys.* **122**, 244322 (2005).
- ³⁶A. N. Panda and N. Sathyamurthy, *J. Chem. Phys.* **122**, 054304 (2005).
- ³⁷V. Aquilanti, G. Capecchi, S. Cavalli, D. D. Fazio, P. Palmieri, C. Puzzarini, A. Aguilar, X. Gimenez, and J. M. Lucas, *Chem. Phys. Lett.* **318**, 619 (2000).
- ³⁸J. D. Kress, R. B. Walker, and E. F. Hayes, *J. Chem. Phys.* **93**, 8085 (1990).
- ³⁹P. Palmieri, C. Puzzarini, V. Aquilanti, G. Capecchi, S. Cavalli, D. D. Fazio, A. Aguilar, X. Gimenez, and J. M. Lucas, *Mol. Phys.* **98**, 1839 (2000).
- ⁴⁰X. N. Tang, H. Xu, T. Zhang, C. Y. Ng, Y. Chiu, R. A. Dressler, and D. J. Levandier, *J. Chem. Phys.* **122**, 164301 (2005).
- ⁴¹D. H. Zhang, *Theory and Application of Quantum Molecular Dynamics* (World Scientific, Singapore, 1999).
- ⁴²R. T. Pack, *J. Chem. Phys.* **60**, 633 (1974).
- ⁴³P. McGuire and D. J. Kouri, *J. Chem. Phys.* **60**, 2488 (1974).
- ⁴⁴T. S. Chu and K. L. Han, *J. Phys. Chem. A* **109**, 2050 (2005).
- ⁴⁵T. S. Chu, Y. Zhang, and K. L. Han, *Int. Rev. Phys. Chem.* **25**, 201 (2006).
- ⁴⁶J. A. Fleck, Jr., J. R. Morris, and M. D. Feit, *Appl. Phys.* **10**, 129 (1976).
- ⁴⁷P. J. Chantry, *J. Chem. Phys.* **55**, 2746 (1971).
- ⁴⁸R. D. Levine and R. B. Bernstein, *J. Chem. Phys.* **56**, 2281 (1972).
- ⁴⁹C. Rebick and R. D. Levine, *J. Chem. Phys.* **58**, 3942 (1973).
- ⁵⁰D. R. McLaughlin and D. L. Thompson, *J. Chem. Phys.* **70**, 2748 (1979).